



UNIVERSIDADE ESTADUAL DE CAMPINAS
SISTEMA DE BIBLIOTECAS DA UNICAMP
REPOSITÓRIO DA PRODUÇÃO CIENTIFICA E INTELECTUAL DA UNICAMP

Versão do arquivo anexado / Version of attached file:

Versão do Editor / Published Version

Mais informações no site da editora / Further information on publisher's website:

<https://pos.sissa.it/444/305>

DOI: 10.22323/1.444.0305

Direitos autorais / Publisher's copyright statement:

©2024 by Sissa Medialab. All rights reserved.

DIRETORIA DE TRATAMENTO DA INFORMAÇÃO

Cidade Universitária Zeferino Vaz Barão Geraldo
CEP 13083-970 – Campinas SP
Fone: (19) 3521-6493
<http://www.repositorio.unicamp.br>

A Novel Tool for the Absolute End-to-End Calibration of Fluorescence Telescopes – The XY-Scanner

Christoph M. Schäfer^{a,*} for the Pierre Auger Collaboration^b

^a*Karlsruhe Institute of Technology , Institute for Astroparticle Physics, Germany*

^b*Observatorio Pierre Auger, Av. San Martín Norte 304, 5613 Malargüe, Argentina*

Full author list: https://www.auger.org/archive/authors_icrc_2023.html

E-mail: spokespersons@auger.org

The Pierre Auger Observatory uses 27 large-aperture wide-angle Schmidt telescopes to measure the longitudinal profile of air showers using the air-fluorescence technique. Up to the year 2013, the absolute calibration of the telescopes was performed by mounting a uniform large-diameter light source on each of the telescopes and illuminating the entire aperture with a known photon flux. Due to the high amount of work and person-power required, this procedure was only carried out roughly once every three years, and a relative calibration was performed every night to track short-term changes. Since 2013, only the relative calibration has been performed. In this paper, we present a novel tool for the absolute end-to-end calibration of the fluorescence detectors, the XY-Scanner. The XY-Scanner uses a portable integrating sphere as a light source, which has been absolutely calibrated. This light source is installed onto a motorized rail system and moved across the aperture of each telescope. We mimic the illumination of the entire aperture by flashing the light source at ~ 1700 positions evenly distributed across the telescope aperture. For the absolute calibration of the light source, we built a dedicated setup that uses a NIST-calibrated photodiode to measure the average photon flux and a PMT to track the pulse-to-pulse stability. We present the laboratory setups used to study the characteristics of the employed light sources and discuss the inter-calibration between selected telescopes.

38th International Cosmic Ray Conference (ICRC2023)
26 July – 3 August, 2023
Nagoya, Japan



*Speaker

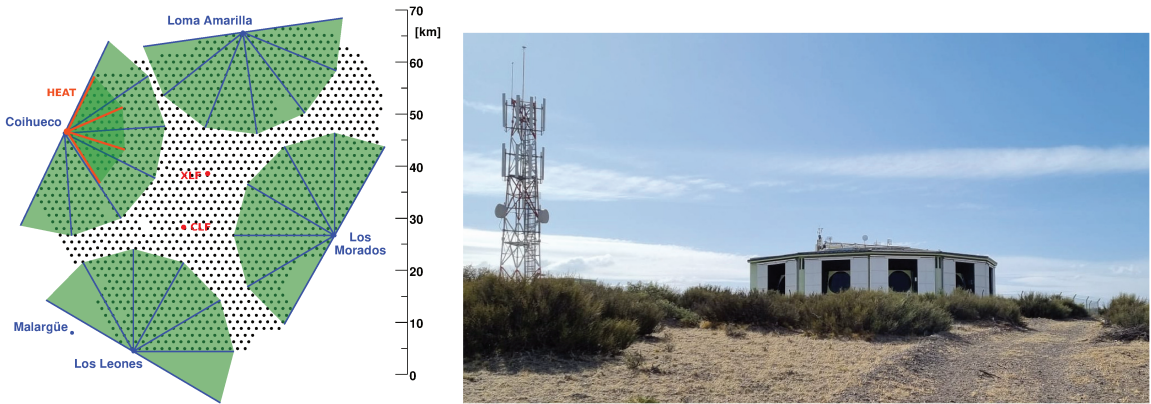


Figure 1: *Left:* Illustration of the Pierre Auger Observatory. Black dots represent SD stations. The field-of-view of the 27 FD telescopes are marked in green. *Right:* Photograph of the Coihueco FD building hosting six telescopes. Communication tower is visible in the left.

1. Introduction

The Pierre Auger Observatory [1] is constructed as a hybrid cosmic-ray observatory combining a surface-detector array (SD) with a system of air-fluorescence telescopes (FD) [2]. The SD employs 1660 self-sufficient water-Cherenkov detector stations distributed across an area of $\sim 3000 \text{ km}^2$. Each black dot on the left side of Fig. 1 represents one SD station. On the edge of the SD array 27 large-aperture fluorescence telescopes are installed on four different sites. These telescopes build the FD. The edges of the field of views of the individual telescopes are marked by the blue lines in the illustration on the left side of Fig. 1. While the SD samples particle reaching the ground, we use the FD to observe the fluorescence light emitted by nitrogen above the array, induced by traversing charged shower particles. We analyze the FD observations to reconstruct the longitudinal shower profile and estimate the energy of the primary cosmic-ray particle as the integral of the profile. Due to the rather low duty cycle of the FD, we use the correlation between the FD energy and a shower-size parameter measured by the SD to perform an energy calibration of the FD. For an accurate energy calibration of the Pierre Auger Observatory, it is therefore mandatory to know the exact conversion between a captured signal in the FD telescope camera and the flux of incident photons.

Up to the year 2013, we performed the absolute end-to-end calibration of the FD telescopes with a uniform large-diameter light source, the so-called *drum* [3, 4]. Since this method of calibration is very demanding in person-power and time required to perform measurements, such measurements were discontinued in 2013. Since then we rely on a nightly relative calibration of the telescope cameras.

2. XY-Scanner

We developed a novel tool to absolutely calibrate the fluorescence telescopes of the Pierre Auger Observatory – the *XY-Scanner*. The XY-Scanner employs a portable and absolutely calibrated light source, which we mount onto a motorized rail system. As light sources we use modified general-purpose integrating spheres (Ulbricht spheres), which are equipped with an LED emitting at a

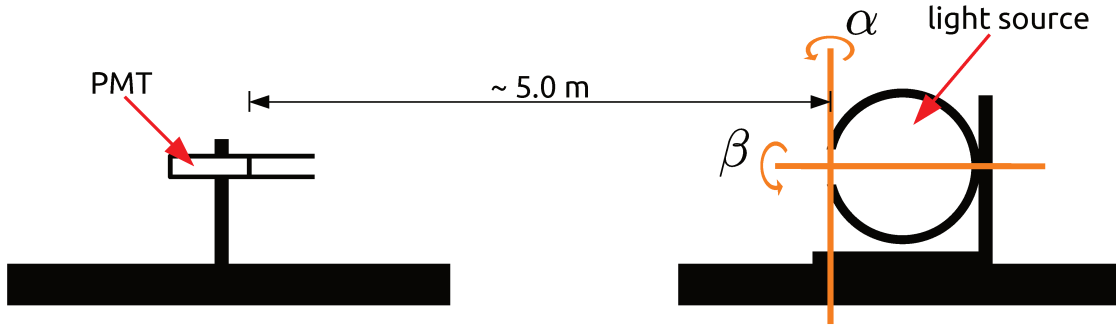


Figure 2: Schematics of the laboratory setup to characterize the angular emission of the light sources.

wavelength of 365 nm. Due to internal reflections within the integrating sphere, its exit port appears as a Lambertian source.

A summary of the XY-Scanner setup and the measuring procedure was presented at the last ICRC in 2021 [5] and a detailed description of the system is given in Ref. [6]. We give here only a very brief description of the system.

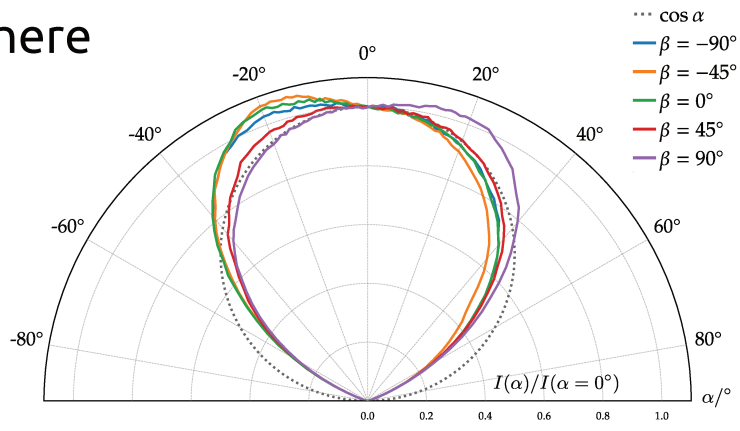
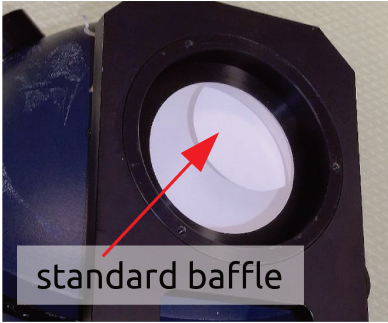
The rail system consists of two vertical linear stages, which are permanently installed onto the aperture of each FD telescope. With some delay due to the global pandemic, we completed equipping all 27 telescopes of the observatory with such rail systems in spring 2023. A horizontal axis is only mounted for XY-Scanner measurements and otherwise stored inside the telescope building. For calibration measurements, we drive the light source to ~ 1700 evenly distributed positions on the scanner. At each position, the light source emits a short light pulse and we capture the total signal collected in the telescope camera. Depending on the distance between light source positions (step size), the total number of positions and thus the total actually illuminated area varies. Since the readout of the entire FD camera takes slightly longer than ~ 1 s, we made a compromise between the illuminated area and the required measuring time. We decided on a step size of 6 cm, which results in a measuring time of less than ~ 45 min per telescope, while still $\sim 65\%$ of the telescope aperture is actually illuminated.

We then combine (a) the total signal collected by the telescope for all positions of the light source, (b) corrections we obtain from ray-traced simulations of the light source and telescope, and (c) detailed studies of the light source emission characteristics to estimate an absolute end-to-end calibration constant for each pixel-PMT of the telescope camera. Combining all contributing uncertainties we are able to reach a total uncertainty of less than 4.5% on the absolute calibration estimated from XY-Scanner measurements.

3. Angular Emission Characteristics of Light Sources

We developed a laboratory setup to estimate the angular emission characteristics of the calibration light sources. For this setup, the light source is mounted onto a combination of motorized rotation stages, which allows us to rotate the source around two independent axes. The first axis is the vertical, going through the midpoint of the exit port, which rotation is denoted by an angle α . The second rotation is around the optical axis of the light source and is labeled β . A schematic

1. Generation Sphere



2. Generation Sphere

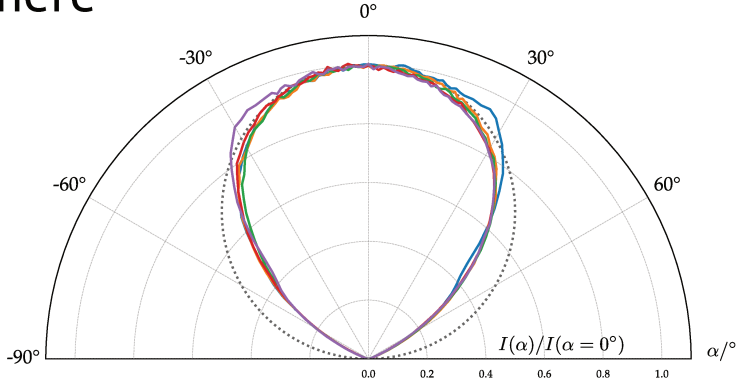
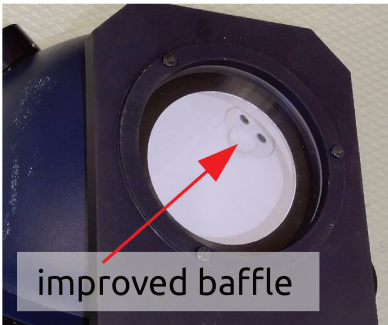


Figure 3: Measurements of the angular emission characteristics of the two generations of integrating-sphere light sources.

drawing of the setup is shown in Fig. 2. Within this figure the rotation axes are indicated by orange lines. At a distance of ~ 5 m a PMT observes the emission from the light source. We choose this particular distance so that the laboratory PMT covers approximately the same solid angle as a pixel-PMT of the FD telescope camera. This setup allows us to directly measure the angular emission of all light sources by observing the source under different viewing angles (α, β) with one single PMT.

Fig. 3 shows the measured angular emission profiles of the two integrating-sphere light sources employed by the XY-Scanner. For the first generation of light sources, we observe a deviation from an ideal Lambertian emitter on the order of $\sim 10\%$. This deviation is induced by the baffle installed in this integrating sphere, as indicated in the top-left photograph of Fig. 3. A baffle is a structural element included in the integrating spheres to prohibit photons emitted from the LED from directly leaving the sphere without any internal reflections. For the second-generation light sources we replaced the large baffle with a smaller one, resulting in a closer agreement between the measured angular emission profile and an ideal Lambertian source. See the bottom row of Fig. 3.

In addition, we implemented the measured angular emission of the two light sources into the XY-Scanner simulation and compared the results of the simulation with measurements at the FD telescopes. We present the results of this comparison in Fig. 4. Therein the top-left plot shows the ratio between the pixel signals captured during two XY-Scanner measurements performed at

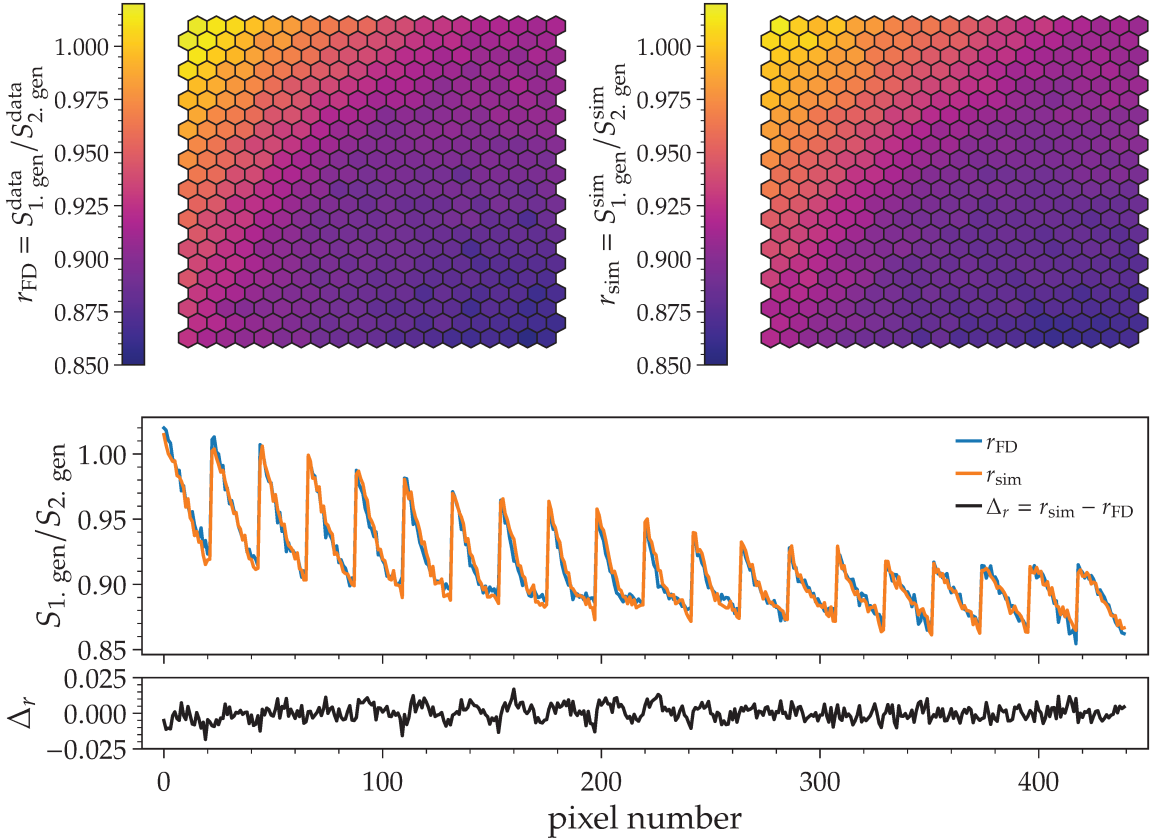


Figure 4: Top-left: Ratio of the FD pixel signals for XY-Scanner measurements employing either of the two integrating-sphere light sources. Top-right: Similar to the left plot, but the results of simulations are shown. Bottom: Shown is the same data as in the top plots, but as a function of the pixel number. Difference Δr between FD measurement and simulation is attached below.

a FD telescope and employing the two different generations of light sources. The top-right plot shows the results of simulating the very same conditions, including the angular source emission as discussed above. In the bottom plots, we show again the ratios from the real FD measurements r_{FD} and simulations r_{sim} as a function of pixel number. Additionally, we show a plot of the difference between measurement and simulation below. We observe a maximal difference of less than 2% while the mean difference is compatible with zero, which we interpret as a validation of our laboratory setup and simulation chain.

4. Absolute Calibration of Light Sources

For the absolute calibration of the light sources we setup and are operating two calibration benches, which are installed at two different institutes. The setups are located at the Bergische Universität Wuppertal (BUW) and the Karlsruhe Institute of Technology (KIT). Since both setups rely on a similar working principle, we focus the following discussion on the setup at KIT.

In Fig. 5 a photograph of this absolute light-source calibration setup is shown. The setup is entirely installed within a light-tight enclosure. To measure the emitted photon flux from the source

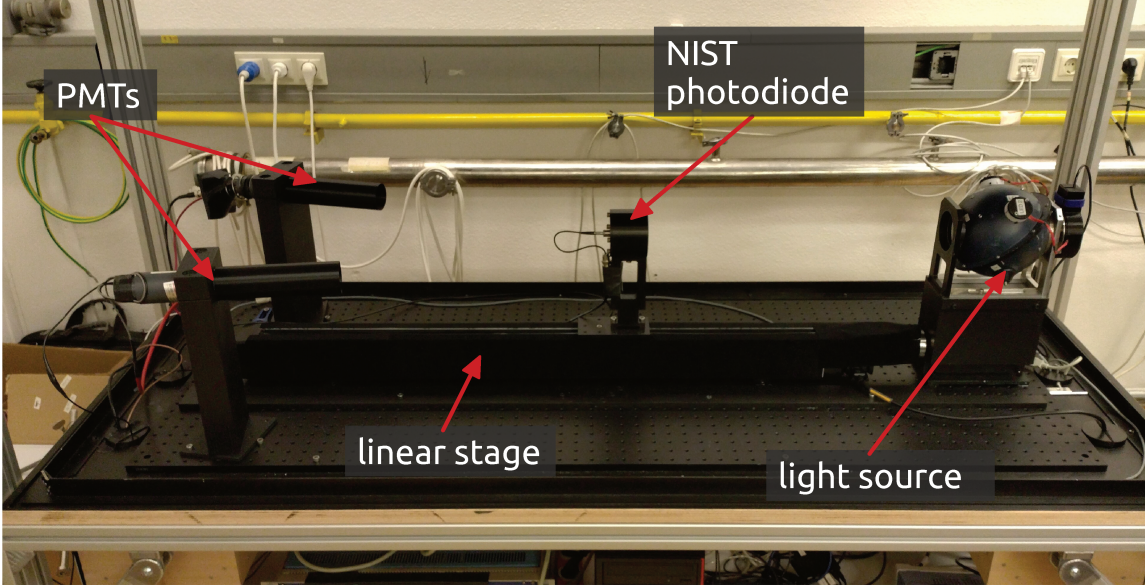


Figure 5: Photograph of one of the setups to absolutely calibrate the light sources of the XY-Scanner. All important components are labeled.

we employ a NIST absolutely-calibrated photodiode. We installed the photodiode on a motorized linear stage, which allows us to change the distance between the source and detector without breaking the light-tightness of the setup. The employed photodiode is designed to be operated with a constant illumination, however for the calibration of the FD telescopes we need to operate the light source in a pulsed mode. Furthermore, we are limited to a maximal flashing frequency of ~ 1 Hz due to the time needed to read out the 440 pixel-PMTs of a telescope camera. We overcame this issue by increasing the flashing frequency for the source calibration and thus nearly constantly illuminating the photodiode. By including two PMTs into the setup, which can resolve each individual light pulse from the source, we are able to correct frequency-dependend intensity variations of the light source.

We calibrated both integrating-sphere light sources in both absolute-calibration setups and obtained compatible results. Depending on the setup we reach an uncertainty of the estimated photon flux emitted from the sources between $\sim 2.8\%$ and $\sim 3.5\%$. We are currently working on upgrading our calibration setups, which will probably reduce the uncertainties on the source calibration measurements even further.

5. Comparison with Night-Sky-Brightness Method

Out of the 27 FD telescopes of the Pierre Auger Observatory, three telescopes take on a special role. These three High Elevation Auger Telescopes (HEAT) can be tilted and thus their field of view covers higher elevation angles than the standard telescopes. HEAT is located close (~ 150 m) to the FD site of Coihueco in the North-West of the observatory. The location of HEAT is drawn on the map in the left part of Fig. 1. We can use a combination of the HEAT and the standard FD telescopes at Coihueco to observe a larger fraction of the longitudinal profiles of deposited energy

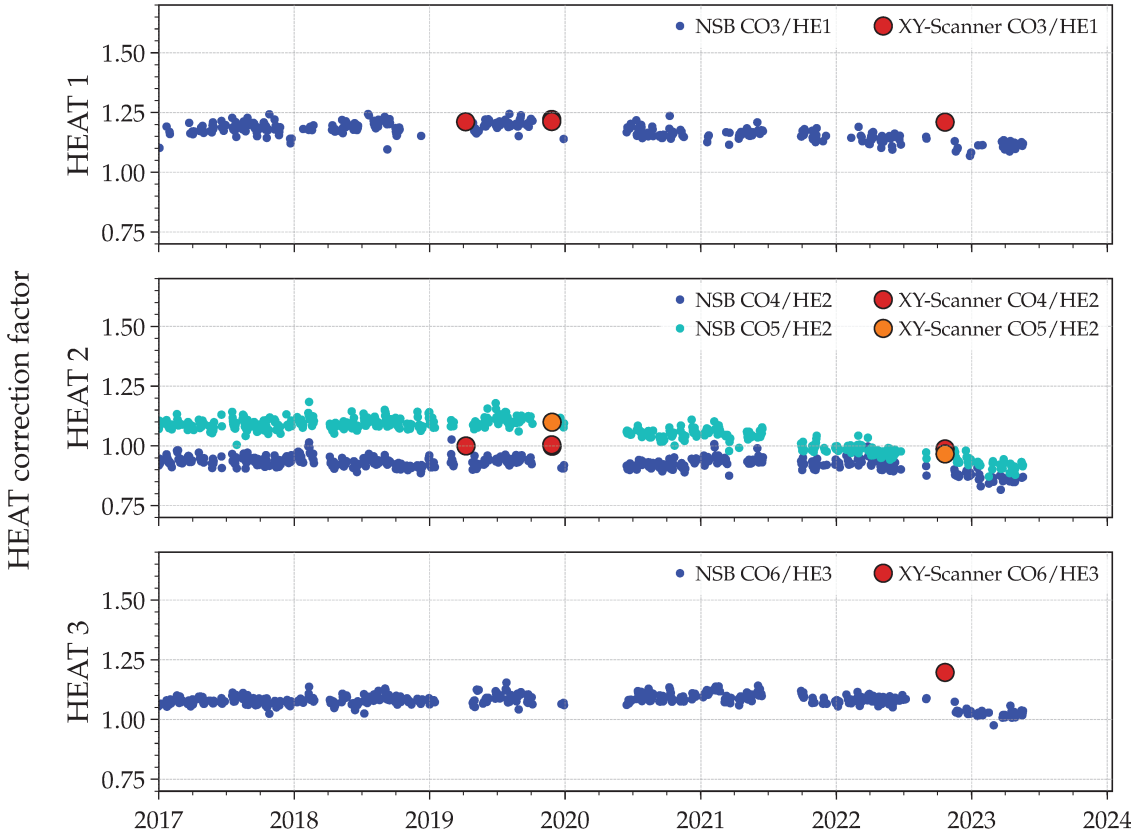


Figure 6: Inter-calibration between the three telescopes of HEAT and the corresponding Coihueco telescopes. Blue and cyan data points represent the NSB method. Results from XY-Scanner measurements are plotted in red and orange.

by air showers. Therefore, the inter-calibration between the telescopes of HEAT and Coihueco is of special interest.

We make use of the continuous estimation of the Night Sky Brightness (NSB) by the HEAT and Coihueco telescopes to monitor their inter-calibration [7]. Due to historic reasons, we adjust the calibration of HEAT to the corresponding Coihueco telescopes. The estimated HEAT correction factors are stored in a database and requested for event reconstruction.

In the following, we present a comparison between the HEAT-Coihueco inter-calibrations obtained from analyzing the NSB and the measurements performed with the XY-Scanner. Note that the XY-Scanner measurements and the NSB observations are independent methods.

We estimate the total signal captured during a complete XY-Scanner measurement as the sum of the calibrated pixel signals for all positions of the light source on the scanning grid. Since the telescopes are designed and constructed in an almost identical way, we can directly calculate the inter-calibration factors between telescopes as the ratio between the signals captured by the corresponding telescopes.

Fig. 6 shows the HEAT correction factors estimated by the NSB method [7] as blue and cyan markers, together with the XY-Scanner measurements depicted as red and orange markers. The

three panels of Fig. 6 show the inter-calibration for the three telescopes of HEAT.

The inter-calibration factors obtained from the XY-Scanner measurements are of the same order as the HEAT correction factors obtained from the NSB observations. Therefore, we give an independent validation of the HEAT correction factors obtained via the NSB analysis.

6. Conclusion and Outlook

In this proceeding, we briefly introduced the XY-Scanner, which is a novel and versatile tool for the absolute end-to-end calibration of the fluorescence telescopes operated by the Pierre Auger Observatory. The setup and the measuring procedure were already presented at the last ICRC in 2021 and are summarized in Refs. [5, 6]. We finished the installation of XY-Scanner systems on all 27 FD telescopes of the observatory in early 2023.

We focused this proceeding on the measurements we performed in the laboratory to accurately study the light-source characteristics. We designed and built two setups to (a) measure the angular emission profiles and (b) estimate the absolute calibration of the employed light sources. For the second case, we installed two independent calibration setups at different institutes, which provide us with necessary redundancy and cross checks.

By including the measured angular emission characteristics of the different light sources into our ray-traced simulations, we observe an excellent agreement between the simulated and the actual (at an FD telescope performed) XY-Scanner measurements.

Furthermore, we used the measurements performed with the XY-Scanner at the FD telescopes to give an independent validation of the inter-calibration between telescopes obtained from analyzing the night-sky-background observations.

We plan to provide a novel absolute end-to-end calibration of all FD telescopes of the Pierre Auger Observatory in the foreseeable future. On a longer time scale, we aim to perform the XY-Scanner calibration campaigns on a yearly basis.

References

- [1] A. Aab et al. [Pierre Auger], *Nucl. Instrum. Meth. A* **798** (2015) 172–213, [[1502.01323](#)].
- [2] J. Abraham et al. [Pierre Auger], *Nucl. Instrum. Meth. A* **620** (2010) 227–251, [[0907.4282](#)].
- [3] J.T. Brack et al., *Astropart. Phys.* **20** (2004) 653.
- [4] J.T. Brack et al., *JINST* **8** (2013) P05014, [[1305.1329](#)].
- [5] C. M. Schäfer et al. [Pierre Auger], *PoS (ICRC2021)* 220.
- [6] C. M. Schäfer, *PhD Thesis (2023)*, Karlsruhe Institute of Technology (KIT).
- [7] A. Segreto et al. [Pierre Auger], these proceedings, *PoS (ICRC2023)* 276.

The Pierre Auger Collaboration



PIERRE
AUGER
OBSERVATORY

- A. Abdul Halim¹³, P. Abreu⁷², M. Aglietta^{54,52}, I. Allekotte¹, K. Almeida Cheminant⁷⁰, A. Almela^{7,12}, R. Aloisio^{45,46}, J. Alvarez-Muñiz⁷⁹, J. Ammerman Yebra⁷⁹, G.A. Anastasi^{54,52}, L. Anchordoqui⁸⁶, B. Andrada⁷, S. Andringa⁷², C. Aramo⁵⁰, P.R. Araújo Ferreira⁴², E. Arnone^{63,52}, J.C. Arteaga Velázquez⁶⁷, H. Asorey⁷, P. Assis⁷², G. Avila¹¹, E. Avocone^{57,46}, A.M. Badescu⁷⁵, A. Bakalova³², A. Balaceanu⁷³, F. Barbato^{45,46}, A. Bartz Mocellin⁸⁵, J.A. Bellido^{13,69}, C. Berat³⁶, M.E. Bertaina^{63,52}, G. Bhatta⁷⁰, M. Bianciotto^{63,52}, P.L. Biermann^h, V. Binet⁵, K. Bismarck^{39,7}, T. Bister^{80,81}, J. Biteau³⁷, J. Blazek³², C. Bleve³⁶, J. Blümer⁴¹, M. Boháčová³², D. Boncioli^{57,46}, C. Bonifazi^{8,26}, L. Bonneau Arbeletche²¹, N. Borodai⁷⁰, J. Brack^j, P.G. Brichetto Orchera⁷, F.L. Brieckle⁴², A. Bueno⁷⁸, S. Buitink¹⁵, M. Buscemi^{47,61}, M. Büsken^{39,7}, A. Bwembya^{80,81}, K.S. Caballero-Mora⁶⁶, S. Cabana-Freire⁷⁹, L. Caccianiga^{59,49}, I. Caracas³⁸, R. Caruso^{58,47}, A. Castellina^{54,52}, F. Catalani¹⁸, G. Cataldi⁴⁸, L. Cazon⁷⁹, M. Cerda¹⁰, A. Cermenati^{45,46}, J.A. Chinellato²¹, J. Chudoba³², L. Chytka³³, R.W. Clay¹³, A.C. Cobos Cerutti⁶, R. Colalillo^{60,50}, A. Coleman⁹⁰, M.R. Coluccia⁴⁸, R. Conceição⁷², A. Condorelli³⁷, G. Consolati^{49,55}, M. Conte^{56,48}, F. Convenga⁴¹, D. Correia dos Santos²⁸, P.J. Costa⁷², C.E. Covault⁸⁴, M. Cristinziani⁴⁴, C.S. Cruz Sanchez³, S. Dasso^{4,2}, K. Daumiller⁴¹, B.R. Dawson¹³, R.M. de Almeida²⁸, J. de Jesús^{7,41}, S.J. de Jong^{80,81}, J.R.T. de Mello Neto^{26,27}, I. De Miti^{45,46}, J. de Oliveira¹⁷, D. de Oliveira Franco²¹, F. de Palma^{56,48}, V. de Souza¹⁹, E. De Vito^{56,48}, A. Del Popolo^{58,47}, O. Deligny³⁴, N. Denner³², L. Deval^{41,7}, A. di Matteo⁵², M. Dobre⁷³, C. Dobrigkeit²¹, J.C. D'Olivo⁶⁸, L.M. Domingues Mendes⁷², J.C. dos Anjos, R.C. dos Anjos²⁵, J. Ebr³², F. Ellwanger⁴¹, M. Emam^{80,81}, R. Engel^{39,41}, I. Epicoco^{56,48}, M. Erdmann⁴², A. Etchegoyen^{7,12}, C. Evoli^{45,46}, H. Falcke^{80,82,81}, J. Farmer⁸⁹, G. Farrar⁸⁸, A.C. Fauth²¹, N. Fazzini^e, F. Feldbusch⁴⁰, F. Fenu^{41,d}, A. Fernandes⁷², B. Fick⁸⁷, J.M. Figueira⁷, A. Filipčič^{77,76}, T. Fitoussi⁴¹, B. Flaggs⁹⁰, T. Fodran⁸⁰, T. Fujii^{89,f}, A. Fuster^{7,12}, C. Galea⁸⁰, C. Galelli^{59,49}, B. García⁶, C. Gaudu³⁸, H. Gemmeke⁴⁰, F. Gesualdi^{7,41}, A. Gherghel-Lascu⁷³, P.L. Ghia³⁴, U. Giaccari⁴⁸, M. Giammarchi⁴⁹, J. Glombitzka^{42,g}, F. Gobbi¹⁰, F. Gollan⁷, G. Golup¹, M. Gómez Berisso¹, P.F. Gómez Vitale¹¹, J.P. Gongora¹¹, J.M. González¹, N. González⁷, I. Goos¹, D. Góra⁷⁰, A. Gorgi^{54,52}, M. Gottowik⁷⁹, T.D. Grubb¹³, F. Guarino^{60,50}, G.P. Guedes²², E. Guido⁴⁴, S. Hahn³⁹, P. Hamal³², M.R. Hampel⁷, P. Hansen³, D. Harari¹, V.M. Harvey¹³, A. Haungs⁴¹, T. Hebbeker⁴², C. Hojvat^e, J.R. Hörandel^{80,81}, P. Horvath³³, M. Hrabovský³³, T. Huege^{41,15}, A. Insolia^{58,47}, P.G. Isar⁷⁴, P. Janecek³², J.A. Johnsen⁸⁵, J. Jurysek³², A. Kääpä³⁸, K.H. Kampert³⁸, B. Keilhauer⁴¹, A. Khakurdikar⁸⁰, V.V. Kizakke Covilakam^{7,41}, H.O. Klages⁴¹, M. Kleifges⁴⁰, F. Knapp³⁹, N. Kunka⁴⁰, B.L. Lago¹⁶, N. Langner⁴², M.A. Leigui de Oliveira²⁴, Y Lema-Capeans⁷⁹, V. Lenok³⁹, A. Letessier-Selvon³⁵, I. Lhenry-Yvon³⁴, D. Lo Presti^{58,47}, L. Lopes⁷², L. Lu⁹¹, Q. Luce³⁹, J.P. Lundquist⁷⁶, A. Machado Payeras²¹, M. Majercakova³², D. Mandat³², B.C. Manning¹³, P. Mantsch^e, S. Marafico³⁴, F.M. Mariani^{59,49}, A.G. Mariazzi³, I.C. Mariş¹⁴, G. Marsella^{61,47}, D. Martello^{56,48}, S. Martinelli^{41,7}, O. Martínez Bravo⁶⁴, M.A. Martins⁷⁹, M. Mastrodicasa^{57,46}, H.J. Mathes⁴¹, J. Matthews^a, G. Matthiae^{62,51}, E. Mayotte^{85,38}, S. Mayotte⁸⁵, P.O. Mazur^e, G. Medina-Tanco⁶⁸, J. Meinert³⁸, D. Melo⁷, A. Menshikov⁴⁰, C. Merx⁴¹, S. Michal³³, M.I. Micheletti⁵, L. Miramonti^{59,49}, S. Mollerach¹, F. Montanet³⁶, L. Morejon³⁸, C. Morello^{54,52}, A.L. Müller³², K. Mulrey^{80,81}, R. Mussa⁵², M. Muzio⁸⁸, W.M. Namasaka³⁸, S. Negi³², L. Nellen⁶⁸, K. Nguyen⁸⁷, G. Nicora⁹, M. Niculescu-Oglintzaru⁷³, M. Niechciol⁴⁴, D. Nitz⁸⁷, D. Nosek³¹, V. Novotny³¹, L. Nožka³³, A. Nucita^{56,48}, L.A. Núñez³⁰, C. Oliveira¹⁹, M. Palatka³², J. Pallotta⁹, S. Panja³², G. Parente⁷⁹, T. Paulsen³⁸, J. Pawlowsky³⁸, M. Pech³², J. Pěkala⁷⁰, R. Pelayo⁶⁵, L.A.S. Pereira²³, E.E. Pereira Martins^{39,7}, J. Perez Armand²⁰, C. Pérez Bertolli^{7,41}, L. Perrone^{56,48}, S. Petrera^{45,46}, C. Petrucci^{57,46}, T. Pierog⁴¹, M. Pimenta⁷², M. Platino⁷, B. Pont⁸⁰, M. Pothast^{81,80}, M. Pourmohammad Shahvar^{61,47}, P. Privitera⁸⁹, M. Prouza³², A. Puyleart⁸⁷, S. Querchfeld³⁸, J. Rautenberg³⁸, D. Ravignani⁷, M. Reininghaus³⁹, J. Ridky³², F. Riehn⁷⁹, M. Risso⁴⁴, V. Rizi^{57,46}, W. Rodrigues de Carvalho⁸⁰, E. Rodriguez^{7,41}, J. Rodriguez Rojo¹¹, M.J. Roncoroni⁷, S. Rossoni⁴³, M. Roth⁴¹, E. Roulet¹, A.C. Rovero⁴, P. Ruehl⁴⁴, A. Saftoiu⁷³, M. Saharan⁸⁰, F. Salamida^{57,46}, H. Salazar⁶⁴, G. Salina⁵¹, J.D. Sanabria Gomez³⁰, F. Sánchez⁷, E.M. Santos²⁰, E. Santos³²,

F. Sarazin⁸⁵, R. Sarmento⁷², R. Sato¹¹, P. Savina⁹¹, C.M. Schäfer⁴¹, V. Scherini^{56,48}, H. Schieler⁴¹, M. Schimassek³⁴, M. Schimp³⁸, F. Schlüter⁴¹, D. Schmidt³⁹, O. Scholten^{15,i}, H. Schoorlemmer^{80,81}, P. Schovánek³², F.G. Schröder^{90,41}, J. Schulte⁴², T. Schulz⁴¹, S.J. Sciutto³, M. Scornavacche^{7,41}, A. Segreto^{53,47}, S. Sehgal³⁸, S.U. Shivashankara⁷⁶, G. Sigl⁴³, G. Silli⁷, O. Sima^{73,b}, F. Simon⁴⁰, R. Smau⁷³, R. Šmídá⁸⁹, P. Sommers^k, J.F. Soriano⁸⁶, R. Squartini¹⁰, M. Stadelmaier³², D. Stanca⁷³, S. Stanič⁷⁶, J. Stasielak⁷⁰, P. Stassi³⁶, S. Strähnz³⁹, M. Straub⁴², M. Suárez-Durán¹⁴, T. Suomijärvi³⁷, A.D. Supanitsky⁷, Z. Svozilikova³², Z. Szadkowski⁷¹, A. Tapia²⁹, C. Taricco^{63,52}, C. Timmermans^{81,80}, O. Tkachenko⁴¹, P. Tobiska³², C.J. Todero Peixoto¹⁸, B. Tomé⁷², Z. Torrès³⁶, A. Travaini¹⁰, P. Travnicek³², C. Trimarelli^{57,46}, M. Tueros³, M. Unger⁴¹, L. Vaclavek³³, M. Vacula³³, J.F. Valdés Galicia⁶⁸, L. Valore^{60,50}, E. Varela⁶⁴, A. Vásquez-Ramírez³⁰, D. Veberič⁴¹, C. Ventura²⁷, I.D. Vergara Quispe³, V. Verzi⁵¹, J. Vicha³², J. Vink⁸³, J. Vlastimil³², S. Vorobiov⁷⁶, C. Watanabe²⁶, A.A. Watson^c, A. Weindl⁴¹, L. Wiencke⁸⁵, H. Wilczyński⁷⁰, D. Wittkowski³⁸, B. Wundheiler⁷, B. Yue³⁸, A. Yushkov³², O. Zapparrata¹⁴, E. Zas⁷⁹, D. Zavrtanik^{76,77}, M. Zavrtanik^{77,76}

¹ Centro Atómico Bariloche and Instituto Balseiro (CNEA-UNCuyo-CONICET), San Carlos de Bariloche, Argentina

² Departamento de Física and Departamento de Ciencias de la Atmósfera y los Océanos, FCEyN, Universidad de Buenos Aires and CONICET, Buenos Aires, Argentina

³ IFLP, Universidad Nacional de La Plata and CONICET, La Plata, Argentina

⁴ Instituto de Astronomía y Física del Espacio (IAFE, CONICET-UBA), Buenos Aires, Argentina

⁵ Instituto de Física de Rosario (IFIR) – CONICET/U.N.R. and Facultad de Ciencias Bioquímicas y Farmacéuticas U.N.R., Rosario, Argentina

⁶ Instituto de Tecnologías en Detección y Astropartículas (CNEA, CONICET, UNSAM), and Universidad Tecnológica Nacional – Facultad Regional Mendoza (CONICET/CNEA), Mendoza, Argentina

⁷ Instituto de Tecnologías en Detección y Astropartículas (CNEA, CONICET, UNSAM), Buenos Aires, Argentina

⁸ International Center of Advanced Studies and Instituto de Ciencias Físicas, ECyT-UNSAM and CONICET, Campus Miguelete – San Martín, Buenos Aires, Argentina

⁹ Laboratorio Atmósfera – Departamento de Investigaciones en Láseres y sus Aplicaciones – UNIDEF (CITEDEF-CONICET), Argentina

¹⁰ Observatorio Pierre Auger, Malargüe, Argentina

¹¹ Observatorio Pierre Auger and Comisión Nacional de Energía Atómica, Malargüe, Argentina

¹² Universidad Tecnológica Nacional – Facultad Regional Buenos Aires, Buenos Aires, Argentina

¹³ University of Adelaide, Adelaide, S.A., Australia

¹⁴ Université Libre de Bruxelles (ULB), Brussels, Belgium

¹⁵ Vrije Universiteit Brussels, Brussels, Belgium

¹⁶ Centro Federal de Educação Tecnológica Celso Suckow da Fonseca, Petropolis, Brazil

¹⁷ Instituto Federal de Educação, Ciência e Tecnologia do Rio de Janeiro (IFRJ), Brazil

¹⁸ Universidade de São Paulo, Escola de Engenharia de Lorena, Lorena, SP, Brazil

¹⁹ Universidade de São Paulo, Instituto de Física de São Carlos, São Carlos, SP, Brazil

²⁰ Universidade de São Paulo, Instituto de Física, São Paulo, SP, Brazil

²¹ Universidade Estadual de Campinas, IFGW, Campinas, SP, Brazil

²² Universidade Estadual de Feira de Santana, Feira de Santana, Brazil

²³ Universidade Federal de Campina Grande, Centro de Ciencias e Tecnologia, Campina Grande, Brazil

²⁴ Universidade Federal do ABC, Santo André, SP, Brazil

²⁵ Universidade Federal do Paraná, Setor Palotina, Palotina, Brazil

²⁶ Universidade Federal do Rio de Janeiro, Instituto de Física, Rio de Janeiro, RJ, Brazil

²⁷ Universidade Federal do Rio de Janeiro (UFRJ), Observatório do Valongo, Rio de Janeiro, RJ, Brazil

²⁸ Universidade Federal Fluminense, EEIMVR, Volta Redonda, RJ, Brazil

²⁹ Universidad de Medellín, Medellín, Colombia

³⁰ Universidad Industrial de Santander, Bucaramanga, Colombia

- ³¹ Charles University, Faculty of Mathematics and Physics, Institute of Particle and Nuclear Physics, Prague, Czech Republic
- ³² Institute of Physics of the Czech Academy of Sciences, Prague, Czech Republic
- ³³ Palacky University, Olomouc, Czech Republic
- ³⁴ CNRS/IN2P3, IJCLab, Université Paris-Saclay, Orsay, France
- ³⁵ Laboratoire de Physique Nucléaire et de Hautes Energies (LPNHE), Sorbonne Université, Université de Paris, CNRS-IN2P3, Paris, France
- ³⁶ Univ. Grenoble Alpes, CNRS, Grenoble Institute of Engineering Univ. Grenoble Alpes, LPSC-IN2P3, 38000 Grenoble, France
- ³⁷ Université Paris-Saclay, CNRS/IN2P3, IJCLab, Orsay, France
- ³⁸ Bergische Universität Wuppertal, Department of Physics, Wuppertal, Germany
- ³⁹ Karlsruhe Institute of Technology (KIT), Institute for Experimental Particle Physics, Karlsruhe, Germany
- ⁴⁰ Karlsruhe Institute of Technology (KIT), Institut für Prozessdatenverarbeitung und Elektronik, Karlsruhe, Germany
- ⁴¹ Karlsruhe Institute of Technology (KIT), Institute for Astroparticle Physics, Karlsruhe, Germany
- ⁴² RWTH Aachen University, III. Physikalisches Institut A, Aachen, Germany
- ⁴³ Universität Hamburg, II. Institut für Theoretische Physik, Hamburg, Germany
- ⁴⁴ Universität Siegen, Department Physik – Experimentelle Teilchenphysik, Siegen, Germany
- ⁴⁵ Gran Sasso Science Institute, L'Aquila, Italy
- ⁴⁶ INFN Laboratori Nazionali del Gran Sasso, Assergi (L'Aquila), Italy
- ⁴⁷ INFN, Sezione di Catania, Catania, Italy
- ⁴⁸ INFN, Sezione di Lecce, Lecce, Italy
- ⁴⁹ INFN, Sezione di Milano, Milano, Italy
- ⁵⁰ INFN, Sezione di Napoli, Napoli, Italy
- ⁵¹ INFN, Sezione di Roma "Tor Vergata", Roma, Italy
- ⁵² INFN, Sezione di Torino, Torino, Italy
- ⁵³ Istituto di Astrofisica Spaziale e Fisica Cosmica di Palermo (INAF), Palermo, Italy
- ⁵⁴ Osservatorio Astrofisico di Torino (INAF), Torino, Italy
- ⁵⁵ Politecnico di Milano, Dipartimento di Scienze e Tecnologie Aeroespaziali , Milano, Italy
- ⁵⁶ Università del Salento, Dipartimento di Matematica e Fisica "E. De Giorgi", Lecce, Italy
- ⁵⁷ Università dell'Aquila, Dipartimento di Scienze Fisiche e Chimiche, L'Aquila, Italy
- ⁵⁸ Università di Catania, Dipartimento di Fisica e Astronomia "Ettore Majorana", Catania, Italy
- ⁵⁹ Università di Milano, Dipartimento di Fisica, Milano, Italy
- ⁶⁰ Università di Napoli "Federico II", Dipartimento di Fisica "Ettore Pancini", Napoli, Italy
- ⁶¹ Università di Palermo, Dipartimento di Fisica e Chimica "E. Segrè", Palermo, Italy
- ⁶² Università di Roma "Tor Vergata", Dipartimento di Fisica, Roma, Italy
- ⁶³ Università Torino, Dipartimento di Fisica, Torino, Italy
- ⁶⁴ Benemérita Universidad Autónoma de Puebla, Puebla, México
- ⁶⁵ Unidad Profesional Interdisciplinaria en Ingeniería y Tecnologías Avanzadas del Instituto Politécnico Nacional (UPIITA-IPN), México, D.F., México
- ⁶⁶ Universidad Autónoma de Chiapas, Tuxtla Gutiérrez, Chiapas, México
- ⁶⁷ Universidad Michoacana de San Nicolás de Hidalgo, Morelia, Michoacán, México
- ⁶⁸ Universidad Nacional Autónoma de México, México, D.F., México
- ⁶⁹ Universidad Nacional de San Agustín de Arequipa, Facultad de Ciencias Naturales y Formales, Arequipa, Peru
- ⁷⁰ Institute of Nuclear Physics PAN, Krakow, Poland
- ⁷¹ University of Łódź, Faculty of High-Energy Astrophysics, Łódź, Poland
- ⁷² Laboratório de Instrumentação e Física Experimental de Partículas – LIP and Instituto Superior Técnico – IST, Universidade de Lisboa – UL, Lisboa, Portugal
- ⁷³ "Horia Hulubei" National Institute for Physics and Nuclear Engineering, Bucharest-Magurele, Romania
- ⁷⁴ Institute of Space Science, Bucharest-Magurele, Romania
- ⁷⁵ University Politehnica of Bucharest, Bucharest, Romania
- ⁷⁶ Center for Astrophysics and Cosmology (CAC), University of Nova Gorica, Nova Gorica, Slovenia
- ⁷⁷ Experimental Particle Physics Department, J. Stefan Institute, Ljubljana, Slovenia

- ⁷⁸ Universidad de Granada and C.A.F.P.E., Granada, Spain
⁷⁹ Instituto Galego de Física de Altas Enerxías (IGFAE), Universidade de Santiago de Compostela, Santiago de Compostela, Spain
⁸⁰ IMAPP, Radboud University Nijmegen, Nijmegen, The Netherlands
⁸¹ Nationaal Instituut voor Kernfysica en Hoge Energie Fysica (NIKHEF), Science Park, Amsterdam, The Netherlands
⁸² Stichting Astronomisch Onderzoek in Nederland (ASTRON), Dwingeloo, The Netherlands
⁸³ Universiteit van Amsterdam, Faculty of Science, Amsterdam, The Netherlands
⁸⁴ Case Western Reserve University, Cleveland, OH, USA
⁸⁵ Colorado School of Mines, Golden, CO, USA
⁸⁶ Department of Physics and Astronomy, Lehman College, City University of New York, Bronx, NY, USA
⁸⁷ Michigan Technological University, Houghton, MI, USA
⁸⁸ New York University, New York, NY, USA
⁸⁹ University of Chicago, Enrico Fermi Institute, Chicago, IL, USA
⁹⁰ University of Delaware, Department of Physics and Astronomy, Bartol Research Institute, Newark, DE, USA
⁹¹ University of Wisconsin-Madison, Department of Physics and WIPAC, Madison, WI, USA

^a Louisiana State University, Baton Rouge, LA, USA

^b also at University of Bucharest, Physics Department, Bucharest, Romania

^c School of Physics and Astronomy, University of Leeds, Leeds, United Kingdom

^d now at Agenzia Spaziale Italiana (ASI). Via del Politecnico 00133, Roma, Italy

^e Fermi National Accelerator Laboratory, Fermilab, Batavia, IL, USA

^f now at Graduate School of Science, Osaka Metropolitan University, Osaka, Japan

^g now at ECAP, Erlangen, Germany

^h Max-Planck-Institut für Radioastronomie, Bonn, Germany

ⁱ also at Kapteyn Institute, University of Groningen, Groningen, The Netherlands

^j Colorado State University, Fort Collins, CO, USA

^k Pennsylvania State University, University Park, PA, USA

Acknowledgments

The successful installation, commissioning, and operation of the Pierre Auger Observatory would not have been possible without the strong commitment and effort from the technical and administrative staff in Malargüe. We are very grateful to the following agencies and organizations for financial support:

Argentina – Comisión Nacional de Energía Atómica; Agencia Nacional de Promoción Científica y Tecnológica (ANPCyT); Consejo Nacional de Investigaciones Científicas y Técnicas (CONICET); Gobierno de la Provincia de Mendoza; Municipalidad de Malargüe; NDM Holdings and Valle Las Leñas; in gratitude for their continuing cooperation over land access; Australia – the Australian Research Council; Belgium – Fonds de la Recherche Scientifique (FNRS); Research Foundation Flanders (FWO); Brazil – Conselho Nacional de Desenvolvimento Científico e Tecnológico (CNPq); Financiadora de Estudos e Projetos (FINEP); Fundação de Amparo à Pesquisa do Estado de Rio de Janeiro (FAPERJ); São Paulo Research Foundation (FAPESP) Grants No. 2019/10151-2, No. 2010/07359-6 and No. 1999/05404-3; Ministério da Ciência, Tecnologia, Inovações e Comunicações (MCTIC); Czech Republic – Grant No. MSMT CR LTT18004, LM2015038, LM2018102, CZ.02.1.01/0.0/0.0/16_013/0001402, CZ.02.1.01/0.0/0.0/18_046/0016010 and CZ.02.1.01/0.0/0.0/17_049/0008422; France – Centre de Calcul IN2P3/CNRS; Centre National de la Recherche Scientifique (CNRS); Conseil Régional Ile-de-France; Département Physique Nucléaire et Corpusculaire (DNC-IN2P3/CNRS); Département Sciences de l'Univers (SDU-INSU/CNRS); Institut Lagrange de Paris (ILP) Grant No. LABEX ANR-10-LABX-63 within the Investissements d'Avenir Programme Grant No. ANR-11-IDEX-0004-02; Germany – Bundesministerium für Bildung und Forschung (BMBF); Deutsche Forschungsgemeinschaft (DFG); Finanzministerium Baden-Württemberg; Helmholtz Alliance for Astroparticle Physics (HAP); Helmholtz-Gemeinschaft Deutscher Forschungszentren (HGF); Ministerium für Kultur und Wissenschaft des Landes Nordrhein-Westfalen; Ministerium für Wissenschaft, Forschung und Kunst des Landes Baden-Württemberg; Italy – Istituto Nazionale di Fisica Nucleare (INFN); Istituto Nazionale di Astrofisica (INAF); Ministero dell'Università e della Ricerca (MUR); CETEMPS Center of Excellence; Ministero degli Affari Esteri (MAE), ICSC Centro Nazionale di Ricerca in High Performance Computing, Big Data

and Quantum Computing, funded by European Union NextGenerationEU, reference code CN_00000013; México – Consejo Nacional de Ciencia y Tecnología (CONACYT) No. 167733; Universidad Nacional Autónoma de México (UNAM); PAPIIT DGAPA-UNAM; The Netherlands – Ministry of Education, Culture and Science; Netherlands Organisation for Scientific Research (NWO); Dutch national e-infrastructure with the support of SURF Cooperative; Poland – Ministry of Education and Science, grants No. DIR/WK/2018/11 and 2022/WK/12; National Science Centre, grants No. 2016/22/M/ST9/00198, 2016/23/B/ST9/01635, 2020/39/B/ST9/01398, and 2022/45/B/ST9/02163; Portugal – Portuguese national funds and FEDER funds within Programa Operacional Factores de Competitividade through Fundação para a Ciência e a Tecnologia (COMPETE); Romania – Ministry of Research, Innovation and Digitization, CNCS-UEFISCDI, contract no. 30N/2023 under Romanian National Core Program LAPLAS VII, grant no. PN 23/21/01/02 and project number PN-III-P1-1.1-TE-2021-0924/TE57/2022, within PNCDI III; Slovenia – Slovenian Research Agency, grants P1-0031, P1-0385, I0-0033, N1-0111; Spain – Ministerio de Economía, Industria y Competitividad (FPA2017-85114-P and PID2019-104676GB-C32), Xunta de Galicia (ED431C 2017/07), Junta de Andalucía (SOMM17/6104/UGR, P18-FR-4314) Feder Funds, RENATA Red Nacional Temática de Astropartículas (FPA2015-68783-REDT) and María de Maeztu Unit of Excellence (MDM-2016-0692); USA – Department of Energy, Contracts No. DE-AC02-07CH11359, No. DE-FR02-04ER41300, No. DE-FG02-99ER41107 and No. DE-SC0011689; National Science Foundation, Grant No. 0450696; The Grainger Foundation; Marie Curie-IRSES/EPLANET; European Particle Physics Latin American Network; and UNESCO.